Chemical Engineering Journal 155 (2009) 108–114

Contents lists available at ScienceDirect

Chemical Engineering Journal

journal homepage: www.elsevier.com/locate/cej

Cadmium(II) removal from aqueous solution using microporous titanosilicate ETS-10

Elizabeth D. Camarinha [a], Patrícia F. Lito [a], Bruno M. Antunes [a], Marta Otero [b], Zhi Lin [a], João Rocha [a], Eduarda Pereira [b], Armando C. Duarte [b], Carlos M. Silva [a,*]

[a] CICECO, Department of Chemistry, University of Aveiro, Campus Universitário de Santiago, 3810-193 Aveiro, Portugal
[b] CESAM, Department of Chemistry, University of Aveiro, Campus Universitário de Santiago, 3810-193 Aveiro, Portugal

ARTICLE INFO

Article history:
Received 17 February 2009
Received in revised form 29 June 2009
Accepted 1 July 2009

Keywords:
Cadmium
ETS-10
Ion exchange
Kinetic
Isotherm
Nernst–Planck

ABSTRACT

In this work, the removal of Cd^{2+} ions from aqueous solution using microporous titanosilicate ETS-10 was investigated in order to assess its potential as decontaminating agent in tertiary treatments. Accordingly, batch stirred tank experiments were carried out to study the ion exchange kinetics and equilibrium. Results show that pH affects considerably the ion exchange capability of ETS-10: at pH 4 it is 1.567×10^2 eq m^{-3}, at pH 6 it is 3.629×10^3, and no further increment was observed at pH 8. This is an extremely important observation since pH of industrial effluents and other wastewaters rounds 6. Both Langmuir and Langmuir–Freundlich isotherms were fitted to the experimental data measured. The second model performs slightly better as the calculated absolute average deviations show: $AAD_L = 2.94\%$ and $AAD_{LF} = 2.40\%$. Concerning the kinetic behavior, the ion exchange was successfully represented by a Nernst–Planck based model (AAD = 11.9%).

1. Introduction

Heavy metals are well known by their toxicity and tendency to accumulate in the living organisms, causing serious diseases and disorders. Such hazardous effects make their presence in the environment of great concern. Toxic heavy metals are mainly discharged into the aquatic system as industrial wastewaters, endangering soil and water quality. Cadmium is one of most toxic non-essential metals, which affects the action of enzymes and hinders respiration, photosynthesis, transpiration and chlorosis [1]. A wide variety of industries are responsible for cadmium pollution including metal plating, cadmium–nickel batteries, petroleum refining, mining, pigments, stabilizers, alloys, agriculture, and electronics [2,3].

The heavy metal levels in wastewater and drinking water must be reduced to a maximum permissible concentration [4,5]. The removal of toxic metals can be achieved by a variety of processes, such as reverse osmosis, chemical precipitation, ion exchange, solvent extraction, adsorption, chemical oxidation and reduction, and electrodialysis [6,7]. Nonetheless, many of those processes involve high operation costs, are non-effective when treating water with low heavy metal levels and exhibit a difficult sludge disposal [8,9]. On the other hand, ion exchange is generally recognized as the most attractive method for removing contaminants from water due to its relative simplicity of application, cost effectiveness and high efficiency, particularly when treating water with low concentration of heavy metals. However, the cost and the regeneration of adsorbents are limiting factors for its application [6].

Microporous titanosilicates are a family of zeolite-type materials containing titanium atoms incorporated as octahedral units within a tetrahedral siliceous matrix, forming a three-dimensional network of interconnected channels [10]. Each titanium ion present in the framework has an associated charge of −2, which is compensated by extra-framework exchangeable cations, usually Na^+ and K^+. These charge-balancing species, as well as water molecules or other adsorbed molecules, reside in the channels of the structure and may be replaced by other ions. These materials have great potential as catalysts, molecular sieves or ion-exchangers [10]. ETS-10 (Engelhard Corporation titanosilicate number 10) is a synthetic wide pore microporous titanosilicate. Its structure comprises corner-sharing SiO_4 tetrahedra and TiO_6 octahedra linked through bridging oxygen atoms [10,11]. This material exhibits high thermal stability and a disordered structure with excellent diffusion characteristics. A detailed structural characterization of ETS-10 was reported by Anderson et al. [11,12].

A number of titanosilicates have recently been used as ion exchangers for heavy metals removal. For instance, ETS-10 has been shown to have high selectivity for several heavy metals such as Pb^{2+}, Cu^{2+}, Cd^{2+}, Co^{2+}, Mn^{2+}, Zn^{2+} and some radiocations [13–19]. Moreover, Bortun et al. [20] evaluated framework and layered

* Corresponding author. Tel.: +351 234 401549; fax: +351 234 370084.
E-mail address: carlos.manuel@ua.pt (C.M. Silva).

1385-8947/$ – see front matter © 2009 Elsevier B.V. All rights reserved.
doi:10.1016/j.cej.2009.07.015

Nomenclature

AAD	average absolute deviation
C_A	concentration of A in bulk solution [mol m^{-3}]
d	particle diameter [m]
D_{AW}	diffusivity of the solute in solution [m^2 s^{-1}]
D_A,D_B	self-diffusion coefficient of species A and B [m^2 s^{-1}]
D_{AB}	interdiffusion coefficient of the pair A–B [m^2 s^{-1}]
F	Faraday constant [C mol^{-1}]
k_f	convective mass transfer coefficient [m s^{-1}]
K_L	Langmuir parameter
K_{LF}	Langmuir–Freundlich parameter
m	mass of ETS-10 [kg]
n	Langmuir–Freundlich parameter
N_A,N_B	intraparticle molar flux of species A and B [mol (m^2 s)$^{-1}$]
$\bar{q}_A$	average concentration of counter ion A in the particle [mol m^{-3}]
q_A,q_B	molar concentration of counter ions A and B in the particle [mol m^{-3} or eq m^{-3}]
q_{max}	maximum ion exchanger capacity [mol m^{-3} or eq m^{-3}]
Q	ion exchanger capacity [eq m^{-3}]
r	radial position in the particle [m]
R	particle radius, m; % of ion removed relative to equilibrium limit concentrations
$\Re$	gas constant [J mol^{-1} K^{-1}]
Re	$=\varepsilon^{1/3}d^{4/3}/\nu$, Reynolds number
Sc	$=\nu/D$, Schmidt number
Sh	$=k_f d/D$, Sherwood number
t	time [s (and h in figures)]
T	temperature [K]
V_L	volume of solution [m^3]
V_{ETS-10}	volume of ETS-10 [m^3]
y_A,y_B	equivalent fraction of components A and B in the particle
z_A,z_B	charges of components A and B

Greek letters

δ	ratio between diffusivities of B and A
ε	mixer power input per unit of fluid mass [m^2 s^{-3}]
ϕ	electric potential [V]
ν	kinematic viscosity [m^2 s^{-1}]
ρ_{ETS-10}	density of ETS-10
ξ	dimensionless radial position

Subscripts

0	initial condition
A	counter ion initially present in solution (Cd^{2+})
B	counter ion initially present in particle (Na^+)
eq	equilibrium
L	Langmuir
LF	Langmuir–Freundlich
R	solid–liquid interface

titanosilicates for cesium and strontium uptake from contaminated groundwater and wastewater; Decaillon et al. [21] studied the ion exchange selectivity of layered titanosilicate AM-4 toward strontium; Koudsi and Dyer [22] studied a synthetic titanosilicate analog of the mineral penkvilsite-2O, i.e., AM-3, for removal of Cobalt-60; and Lopes et al. [23–25] evaluated the potential of synthetic microporous (ETS-4, ETS-10, and AM-2) and layered (AM-4) titanosilicates for decontamination of natural waters polluted with low mercury levels and Ferreira et al. [26] investigated the ability of ETS-4 to uptake cadmium(II) from aqueous solution. The results obtained have revealed the potential of titanosilicates as decontaminant agents. In this work, the ability of ETS-10 to remove cadmium from aqueous solution is assessed.

The mass transfer description of an adsorptive process is generally of great importance for its design, optimization, and scale-up since in many of these applications the process performance is mass-transfer-limited [27]. The kinetics of ion exchange is frequently described in literature by semiempirical pseudo first- and second-order equations [23,28–36]. However, such models have no theoretical background, which limits their application and extrapolation. Mass transport in dilute ionic systems can be effectively described by the Nernst–Planck equations, which takes into account both the concentration and the electric potential gradients; the last one is induced by the different counter ions mobility [37–40]. An alternative approach concerns the application of the Maxwell–Stefan equations, due to their well-documented advantages in mass transport [41]. Such formalism has been recently adopted to describe Hg^{2+} and Cd^{2+} removal by titanosilicate ETS-4 [42,43]. Under the specific conditions studied, the results revealed that both models describe accurately well the ion exchange process.

In a previous work we studied the applicability of titanosilicate ETS-4 to uptake Cd^{2+} from aqueous solution [26]. In the present work, we explore the ability of microporous titanosilicate ETS-10 to remove Cd^{2+} ions, assessing its potential as a decontaminating agent. pH is an important variable in ion-exchange processes, hence its effect has been studied also. The results of batch experiments performed are modelled using Nernst–Planck equations.

2. Experimental

2.1. Materials and solutions

All chemicals used were of analytical reagent grade and obtained from commercial suppliers without further purification. The certified standard stock solution of cadmium (1001 ± 2 mg L^{-1}) was purchased from Merck.

All glassware to be used with the cadmium solutions were acid-washed prior to use (HNO_3 25%, 12 h followed by HCl 25% another 12 h).

Cadmium solutions were prepared daily by diluting the stock solution to the desired concentrations in high purity water (18 MΩ cm). The stock solution of cadmium(II) is extremely acidic and when it is diluted in 2 L of water, solutions with pH values around 4 are obtained. NaOH was added to these solutions in order to fix them in different pH. The pH remains approximately constant during the experiments even with no buffer solution added.

ETS-10 was synthesized as follow: 2.50 g of KCl, 1.24 g of KOH (85 wt%, Merck), 6.99 g of KF and 11.51 g of NaOH were dissolved in 34.6 g of H_2O. Then, 66.50 g of $TiCl_3$ (15 wt% $TiCl_3$ and 10 wt% HCl, Merck) were added to this solution with vigorously stirring, followed by 79.09 g of sodium silicate solution (25.5–28.5 wt% SiO_2, 7.5–8.5 wt% Na_2O, Merck). Finally, 0.80 g of ETS-10 seeds were added and the mixture was further agitated for 30 min. The mixture was transferred into Teflon-lined autoclave and treated statically at 230 °C for 30 h under autogenous pressure. After fast cooling with flowing water product was filtered, washed with distilled water and dried at 60 °C overnight.

Powder X-ray patterns were recorded on a Philips X'Pert MPD diffractometer with CuKα X-radiation. The morphology and crystal size of the samples were examined using scanning electron microscope (SEM) on a Hitachi S-4100 microscope. In Table 1, most important properties of ETS-10 are shown.

Table 1
Properties of the ETS-10 particles used.

Formula	$[(Na,K)_2TiSi_5O_{13}{\cdot}4H_2O]$
Density ($kg\,m^{-3}$)	1800
Ion exchanger capacity ($eq\,kg^{-1}$)	4.52
Particle diameter (10^{-6} m)	5
Pore diameter (10^{-10} m)	4.9×7.6

2.2. Batch experiments

All experiments were carried out in batch isothermal (295 ± 1 K) conditions in a closed volumetric flask (2×10^{-3} m^3) to avoid evaporation. Known masses of ETS-10 were added to solutions with fixed initial concentration (0.85×10^{-3} $kg\,m^{-3}$), and this time was considered the starting point of the experiment. The experimental conditions may be found in Table 2. An initial solution concentration of 0.85×10^{-3} $kg\,m^{-3}$ was used since it is in the order of magnitude of industrial effluents discharge limits [44].

ETS-10 powders and aqueous solutions were maintained in contact under constant stirring, using a magnetic mixer at 500 rpm with an impeller of 2 cm, until Cd^{2+} concentration remained constant. Several aliquots (10 mL) filtered through a 0.45 μm Acetate Plus Osmonics filter were taken from the vessel along time. The filtrate was adjusted to pH <2 with HCl, stored at 277.15 K, and then analysed by Inductively Coupled Plasma Mass Spectrometry on a Thermo ICP-MS X Series equipped with a Burgener nebuliser. A blank experiment (without ETS-10) was always run as a control, to check that the removal of cadmium occurred by ion-exchange onto ETS-10 and not by adsorption on the vessel walls, for instance.

At pH 6 nine experiments were performed: Exps. 1–8 gave rise to kinetic curves, whereas Exp. 9 was only carried out to measure an additional equilibrium point for the isotherm. At pH 4 nine assays were also accomplished, from which it was only possible to determine the equilibrium, since it was always reached very fast.

The average concentration of sorbed metal at time t, $\bar{q}_A$, was calculated by material balance:

$$\bar{q}_A = \frac{(C_{A,0} - C_A)V_L}{V_{ETS\text{-}10}} \tag{1}$$

where subscript 'A' denotes Cd^{2+}, $C_{A,0}$ is the initial solution concentration, C_A is the solution concentration at time t, V_L is the solution volume, $V_{ETS\text{-}10} = m/\rho_{ETS\text{-}10}$ is the volume of titanosilicate, m is the mass of ETS-10, and $\rho_{ETS\text{-}10}$ is its density.

3. Modelling

The model adopted in this work to describe the batch ion exchange has been already presented in detail in a previous publication [24] dealing with Hg^{2+} removal from aqueous solution using ETS-4. It embodies the following hypothesis: (i) film and intraparticle mass transfer resistances; (ii) spherical solid particles; (iii) perfectly stirred tank; (iv) isothermal operation; (v) liquid and solid volume changes are neglected; (vi) co-ions are excluded from the zeolite particles (Donnan exclusion); (vii) ideal solution behavior.

Ion-exchange may be represented by conventional chemical equilibrium [37]. For the case where the titanosilicate is initially in B (Na^+) form and the counter ion in solution is A (Cd^{2+}), the equilibrium may be represented by:

$$z_A\overline{B^{z_B}} + z_B A^{z_A} \Leftrightarrow z_B\overline{A^{z_A}} + z_A B^{z_B} \tag{2}$$

where z_A and z_B are the electrochemical valences.

In dilute ionic solutions, intraparticle flux of each counter ion can be accurately described by the Nernst–Planck equations [37]:

$$N_A = -D_A\nabla q_A - D_A z_A q_A \frac{F}{\Re T}\nabla\phi \tag{3}$$

$$N_B = -D_B\nabla q_B - D_B z_B q_B \frac{F}{\Re T}\nabla\phi \tag{4}$$

where D_A and D_B are the self-diffusion coefficients of A and B, respectively, q_A and q_B are the molar concentrations of A and B in the particle, F is Faraday constant, $\Re$ is gas constant, T is absolute temperature, ϕ is the electric potential, and ∇ is the gradient operator.

In the development of the model equations, conditions of electroneutrality and nonexistent electric current were assumed:

$$q_A z_A + q_B z_B = Q \tag{5}$$

$$z_A N_A + z_B N_B = 0, \tag{6}$$

where Q is the ion exchanger capacity. The resulting Nernst–Planck equations are presented here as a special form of Fick's first law, in nondimensional form, where a coupled interdiffusion coefficient, D^*_{AB}, appears:

$$N^*_A = -D^*_{AB}\left(\frac{\partial y_A}{\partial \xi}\right), \tag{7}$$

with

$$D^*_{AB} = \frac{\delta(z_A y_A + z_B y_B)}{z_A y_A + \delta z_B y_B} \tag{8}$$

Nondimensional variables are defined as follows:

$$\delta = \frac{D_B}{D_A}, y_A = \frac{z_A q_A}{Q}, \xi = \frac{r}{R}, N^*_A = \frac{z_A R}{Q D_A} N_A \tag{9}$$

where R is the particle radius and r is the radial coordinate.

The material balances in the particle and in the vessel are, respectively:

$$\left(\frac{\partial q_A}{\partial t}\right) = -\frac{1}{r^2}\frac{\partial}{\partial r}(r^2 N_A) \tag{10}$$

and

$$\frac{dC_A}{dt} = -\frac{V_{ETS\text{-}10}}{V_L}\frac{d\,\bar{q}_A}{dt} \tag{11}$$

The average loading per unit particle volume is calculated by:

$$\bar{q}_A = \frac{3}{R^3}\int_0^R r^2 q_A dr \tag{12}$$

Table 2
Experimental conditions studied: Temperature = 295 ± 1 K; Solution volume = 2×10^{-3} m^3; Initial Cd^{2+} concentration = 0.85×10^{-3} $kg\,m^{-3}$.

Number of experiment at pH 6	1	2	3	4	5	6	7	8	9
Mass of ETS-10, (10^{-6} kg)	5	7.5	10	15.2	17.5	20	40	160	6
Type of data measured				Kinetic and equilibrium					Equilibrium

Number of experiment at pH 4	10	11	12	13	14	15	16	17	18
Mass of ETS-10, (10^{-6} kg)	50	75	105	130	160	175	200	230	250
Type of data measured					Equilibrium				

The above differential equations are subjected to the following initial and boundary conditions:

$$t = 0, \quad \begin{cases} q_A = \bar{q}_A = 0 \\ C_A = C_{A,0} \end{cases} \tag{13}$$

$$r = R, \quad q_A = q_{A,R} \tag{14}$$

$$r = 0, \quad \left(\frac{\partial q_A}{\partial r}\right) = 0 \tag{15}$$

The concentration at the interface is determined by the equality of internal and external fluxes, i.e.,

$$N_A\Big|_{r=R} = k_f(C_A - C_{A,R}) \tag{16}$$

where k_f is the convective mass transfer coefficient. For well established agitated systems, k_f may be predicted using correlations which involve generally the Sherwood, Reynolds, Schmidt and Power numbers, and geometrical parameters such as the ratio of impeller to tank diameters, the specific geometry of the impeller, and the geometry of baffling, if any, used to inhibit vortex formation in the vessel. For the particular geometry of our sorption set-up no correlation is available in the literature. Nonetheless, the correlation of Armenate and Kirwan [45] has been adopted to estimate the convective mass transfer coefficient, at least to predict its order of magnitude:

$$Sh = 2 + 0.52Re^{0.52}Sc^{1/3} \tag{17}$$

where $Sh = k_f d/D_{AW}$ is the Sherwood number, $d = 2R$ is the particle diameter, D_{AW} is the solute diffusivity in solution, $Re = \varepsilon^{1/3}d^{4/3}/\nu$ is the Reynolds number, ε is the mixing power input per unit of fluid mass, ν is the kinematic viscosity, and $Sc = \nu/D_{AW}$ is the Schmidt number. This equation is frequently applied to calculate k_f in order to reduce the number of model parameters. Alternatively, it may be used to estimate k_f and compare it with the optimized values from experimental data [46,47]. The equation of Armenate and Kirwan has been chosen due to its simplicity and because it was specifically derived for microparticles in agitated systems. The mixing power was estimated using the correlation of Rushton et al. [48,49] for similar geometries.

To model the ion-exchange behavior, both kinetic and equilibrium have to be simultaneously taken into account. The equilibrium between bulk solution and exchanger are evaluated in this work using Langmuir (L) and Langmuir–Freundlich (LF) isotherms. The Langmuir isotherm can be represented by:

$$q_{A,eq} = \frac{q_{max}K_L C_{A,eq}}{1 + K_L C_{A,eq}} \tag{18}$$

where K_L and q_{max} are its parameters. Langmuir equation has been the most widely used model for heavy metals sorption onto several materials. Langmuir–Freundlich isotherm combines features of both Langmuir and Freundlich models. It is written as:

$$q_{A,eq} = \frac{q_{max}K_{LF}C_{A,eq}^{1/n}}{1 + K_{LF}C_{A,eq}^{1/n}} \tag{19}$$

where q_{max}, $1/n$ and K_{LF} are the parameters involved.

The simultaneous solution model equations gives the concentration of counter ions in the fluid, and their concentration profiles in the solid phase as function of position and time. The model has been solved numerically using the Method of Lines [50] and integrated by the Finite-Difference approach. For that purpose, a program in Matlab has been written to solve the resulting Ordinary Differential Equations (ODEs) with finite-difference approach. Ode15s has been used to integrate these set of ODEs of the initial-value type.

The self-diffusion coefficients and the convective mass transfer coefficient are the model parameters to fit to the experimental data. Accordingly, a first optimization step was performed based on the 'elimination of linear parameters in nonlinear regression' technique due to Lawton and Sylvestre [51]. With this procedure, a reduction of the number of parameters that must be estimated by the iterative procedure is achieved, as well as faster convergence attained. Thus, only two initial guesses have to be provided instead of three: specifically the diffusivities ratio D_A/D_B, and k_f. Finally, an enhancing optimization involving all parameters simultaneously was performed, where the results previously obtained from the above mentioned technique were taken as reliable initial guesses. This optimization technique has been successfully applied elsewhere [51].

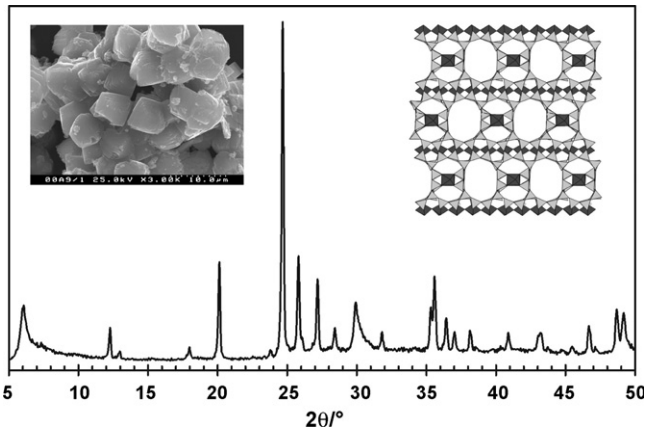

Fig. 1. Powder XRD, SEM image (left) and structure (right) of ETS-10 (polymorph A): black TiO_6 octahedra, grey SiO_4 tetrahedra, water molecules and extra-framework cations not shown, for clarity.

4. Results and discussion

The powder XRD pattern (see Fig. 1) confirms that the ETS-10 sample studied here is of high purity and crystallinity [11,12]. SEM (in Fig. 1) reveals the typical habit of ETS-10 crystals, with a size of *ca.* 5 μm. The right inset in Fig. 1 depicts the structure of ETS-10 (polymorph A), showing the 12-membered ring channel.

Fig. 2 shows the evolution of normalized Cd^{2+} concentration in the fluid along time, measured for different titanosilicate masses at pH 6 (Exps. 1–8 in Table 2). Results follow expected trends, i.e., cadmium removal increases with increasing titanosilicate mass since the extensive ion-exchange capacity is proportional to solid mass. It is evident from Fig. 2 that a fast metal uptake occurs in the first few hours of the process, followed by the characteristic slower removal towards the equilibrium. Such fact is due to the large mass transport driving forces observed at the beginning, since ETS-10 particles are initially free of cadmium.

The equilibrium data at pH 4 (Exps. 10–18 in Table 2) and pH 6 (Exps. 1–9 in Table 2) are presented in Fig. 3. In the case of Exps. 1–8, the isotherm points were calculated averaging the horizontal branch of the curves in Fig. 2, whereas all data measured in Exps. 9–18 correspond directly to equilibrium. As can be noted from Fig. 3, the amount of sorbed Cd^{2+} increases significantly when pH increase from 4 to 6, which is an extremely important result since this is the pH of industrial effluents and other wastewaters. Such behavior can be attributed to the competition between H^+ and Cd^{2+} ions towards the solid sorption sites, which is more pronounced at lower pH values where H^+ concentration is higher. The effect of pH on the removal of metal ions by several exchangers has been investigated. For instance, Lv et al. [15] have observed such a sharp increase for Cd^{2+} and Cu^{2+} on ETS-10, increasing pH from 2.5 to 6. Mishra et al. [52] carried out the uptake of Cd^{2+} on alkali metal titanates, and observed a significant reduction of the sorbed metal

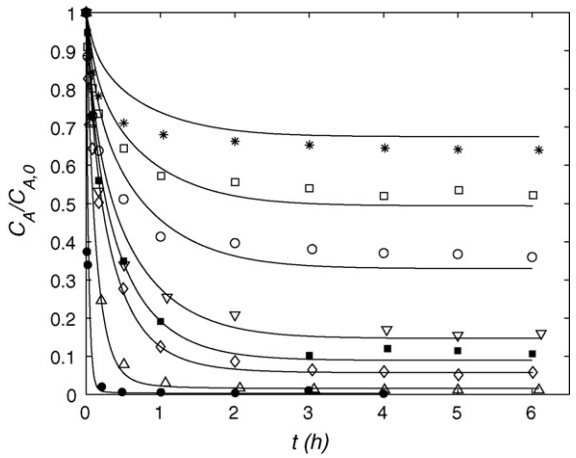

Fig. 2. Normalized concentration of bulk solution versus time: experimental data and modelling (lines). Experimental conditions (see Table 2): (*) Exp. 1; (□), Exp. 2; (○), Exp. 3; (▽), Exp. 4; (■), Exp. 5; (◊) Exp. 6; (Δ) Exp. 7; (●) Exp. 8.

amount by decreasing pH from 10.2 to 3.1. Kocaoba [53] showed that the Cd^{2+} and Pb^{2+} exchange on Amberlite IR 120 resin and dolomite increased when pH goes from 1 to 8. Similar results were also obtained by El-Kamash for Cs^{+} and Sr^{2+} removal on zeolite A [54].

Both Langmuir and Langmuir–Freundlich isotherms were used to fit the experimental equilibrium data obtained at pH 6. In Table 3 the resulting model parameters are listed together with the corresponding average absolute deviations (AAD) found. As may be observed, both isotherms fitted data accurately over the entire range of experimental conditions studied, although the Langmuir–Freundlich model gives slightly better results: AAD_{LF} = 2.40% versus AAD_L = 2.94%. Choi et al. [18] studied the removal of Cu^{2+}, Co^{2+}, Mn^{2+}, and Zn^{2+} ions on ETS-10 and on its variant ETAS-10, and showed that equilibrium were best represented by Langmuir–Freundlich model as well.

Fig. 4 establishes a comparison between our equilibrium data at pH 6 and those available in literature for Cd^{2+} removal for several systems and conditions, namely: Lv et al. [15], ETS-10 at pH 5 and T = 298 K; Ferreira et al. [26], ETS-4 at pH 4 and 295 K; Kocaoba [53], amberlite at pH 5 and 293 K; Sprynskyy et al. [55], clinoptilolite under pH 6.2, at room temperature; and Ok et al. [56], a mixture of a zeolite by-product with Portland ciment (ZeoAds) and activated carbon at pH 5 and T = 298 K. It may be observed that the Cd^{2+} removal by ETS-10 under our experimental conditions significantly surmounts that achieved by the remaining materials. For instance, it is 4 and 14 times higher than that accomplished by

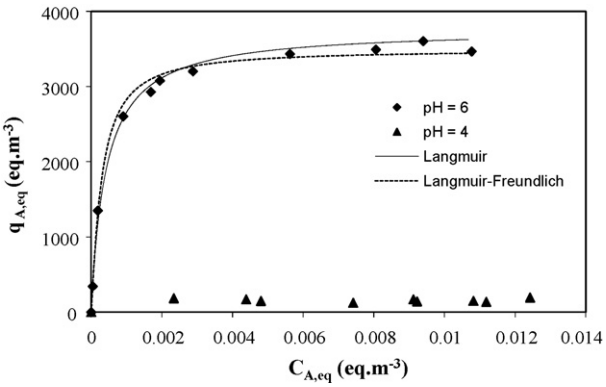

Fig. 3. Equilibrium data at pH 4 and 6 along with Langmuir and Langmuir-Freundlich isotherms fitted at pH 6 (T = 295 K).

Table 3
Langmuir and Langmuir–Freundlich isotherm parameters for pH 6 and average absolute deviations (T = 295 K).

Langmuir			
K_L (m^3 eq^{-1})	q_{max} (eq m^{-3})		ADD (%)
2.322×10^3	3.681×10^3		2.94
Langmuir–Freundlich			
K_{LF} ($m^{3/n}$ eq$^{-1/n}$)	q_{max} (eq m^{-3})	$1/n$	ADD (%)
4.130×10^3	3.629×10^3	1.056	2.40

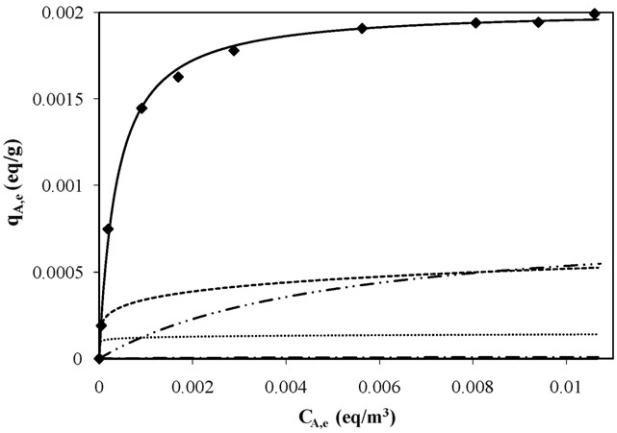

Fig. 4. Comparison between equilibrium data measured in this work (ETS-10, pH 6 and T = 295 K; lozenges) and other isotherms available in literature for ETS-10 and for different solid materials: dash-dot-dotted line: ETS-10 (pH 5 and T = 298 K) [15]; dashed line: ETS-4 (pH 4 and 295 K) [26]; dotted line: amberlite (pH 5 and 293 K) [53]; dash-dotted line: clinoptilolite (pH 6.2, at room temperature) [55]; solid thick line: ZeoAds (pH 5 and T = 298 K) [56]; long dashed line: activated carbon (pH 5 and T = 298 K) [56].

ETS-4 and Amberlite (both at pH 4), and it is notably more effective than clinoptilolite (pH 6.2). Besides, the influence of pH is also emphasized in this figure, as the isotherms at pH 5 and 6 are clearly different.

In Fig. 2 the results obtained with the Nernst–Planck based model are plotted together with experimental data for pH 6 (Exps. 1–8 of Table 2). The calculated parameters (i.e., self-diffusion coefficients and mass transfer coefficient) and the average absolute deviation are listed in Table 4. This figure points out the reliable agreement between modelling and data, corresponding to AAD = 11.9%, even in the transition from steep descent to the horizontal branch, where kinetic curves are frequently difficult to fit. In fact, this may be considered a remarkable result, attending to the number of experimental curves fitted and to the discrepancy in their experimental conditions, namely the mass of ETS-10 used which varies from 5 to 160 mg. Furthermore, as illustrated in Fig. 5, the percentage deviations calculated by Nernst–Planck model are uniformly distributed along concentration.

The optimized self-diffusivities of Cd^{2+} and Na^{+} in ETS-10 were 1.082×10^{-16} 2.319×10^{-15} m^2 s^{-1} respectively. The orders of magnitude of these coefficients are considerably higher than those obtained in a previous work for the same metal ion in ETS-4 (10^{-19} and 10^{-18}, respectively) [26]. This is an expectable result due to

Table 4
Calculated results for the models studied in this work.

Nernst–Planck based model ADD = 11.9%		
D_A (m^2 s^{-1})	D_B (m^2 s^{-1})	k_f (m s^{-1})
1.082×10^{-16}	2.319×10^{-15}	1.628×10^{-4}

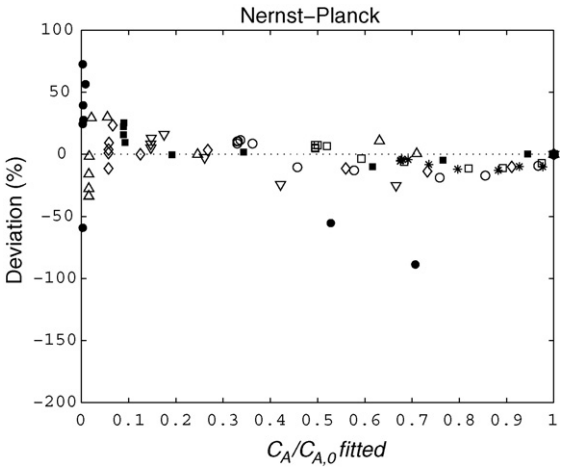

Fig. 5. Plot of the average deviations versus corresponding normalized Cd^{2+} concentration in bulk solution calculated by Nernst–Planck model. Experimental conditions: same as Fig. 2.

the difference between the pore dimensions of both titanosilicates (i.e., 0.49 × 7.6 and 0.3–0.4 nm, respectively). Since ETS-10 pores are wider, cadmium and sodium cations are expected to diffuse through it with higher mobility.

The orders of magnitude of the diffusivities found are consistent with both the small pore diameters of microporous titanosilicates ETS-10 and ETS-4 and the strong and long range nature of the electrostatic interactions. Similar and even smaller values (10^{-17} to 10^{-26} m^2/s) are reported in literature for several ion-exchange systems involving other microporous materials. For instance, apparent diffusion coefficients of 1.8×10^{-17} and 8.0×10^{-18} $m^2\ s^{-1}$ were obtained by Coker and Rees [57] for Ca^{2+} and Mg^{2+}, respectively, in semi-crystalline zeolite Na-A; Brooke and Rees [58] reported interdiffusion diffusivities in the range of 10^{-18} to 10^{-19} $m^2\ s^{-1}$ for the system Na^+/K^+ in shabazite; and Coker and Rees [59] presented interdiffusion coefficients of 2.00×10^{-18} and 6.53×10^{-18} $m^2\ s^{-1}$ for Na^+/Ca^{2+} and Na^+/Mg^{2+} in beryllophosphate-G. Ahmed et al. [60] published an estimated Cd^{2+} apparent diffusion coefficient of 2.84×10^{-23} $m^2\ s^{-1}$ in CaX zeolite.

The convective mass transfer coefficient fitted was $k_f = 1.63 \times 10^{-4}$ m s^{-1}, while that predicted by Armenante and Kirwan's correlation was 1.93×10^{-4} m s^{-1}. Such interesting result validates our optimized value, even though some values used in the correlation were not entirely appropriate, namely: (i) the power was approximately calculated, and (ii) the size of our ETS-10 particles ($d = 5 \times 10^{-6}$ m) is slightly lower than the inferior limit studied by Armenante and Kirwan (range of d: $(6–420) \times 10^{-6}$ m).

5. Conclusions

In this work the removal of Cd^{2+} from aqueous solution using titanosilicate ETS-10 has been investigated carrying out batch stirred tank experiments. The effects of pH and titanosilicate mass have been studied.

Obtained results show that cadmium removal increases with both increasing pH and increasing titanosilicate mass. The amount of sorbed metal by ETS-10 is much higher at pH 6 ($q_{A,max} = 3.629 \times 10^3$ eq m^{-3}) than at pH 4 ($q_{A,max} = 1.567 \times 10^2$ eq m^{-3}), which is a very important result since the pH of industrial effluents and other wastewater is around 6.

Langmuir and Langmuir–Freundlich isotherms were used to fit experimental equilibrium data. Both isotherms provide accurate representation over the range of experimental conditions studied, though Langmuir–Freundlich model performs slightly better: $AAD_{LF} = 2.40\%$ versus $AAD_L = 2.94\%$.

In terms of kinetic behavior, the ion exchange of Cd^{2+} uptake in ETS-10 was successfully described by the proposed Nernst–Planck based model (AAD = 11.9%).

Acknowledgments

Patrícia F. Lito wishes to thank Ph.D. grant provided by Fundação para a Ciência e Tecnologia (Portugal) (SFRH/BD/25580/2005). Authors acknowledge FEDER for financial support.

References

[1] S. Ahmed, S. Chughtai, M.A. Keane, The removal of cadmium and lead from aqueous solution by ion exchange with Na–Y zeolite, Sep. Purif. Technol. 13 (1998) 57–64.
[2] B. Biskup, B. Subotic, Removal of heavy metal ions from solutions by means of zeolites: I. Thermodynamics of the exchange processes between cadmium ions from solution and sodium ions from zeolite A, Sep. Sci. Technol. 33 (4) (1998) 449–466.
[3] V.J. Inglezakis, M.D. Loizidou, H.P. Grigoropoulou, Equilibrium and kinetic ion exchange studies of Pb^{2+}, Cr^{3+}, Fe^{3+} and Cu^{2+} on natural clinoptilolite, Water Res. 36 (2002) 2784–2792.
[4] World Health Organization, Guidelines for Drinking-Water Quality: Incorporating First Addendum, vol. 1, Recommendations, 3rd ed., ISBN 92 4 154696 4, 2006.
[5] G. Bereket, A.Z. Aroguz, M.Z. Ozel, Removal of Pb(II), Cd(II), Cu(II) and Zn(II) from aqueous solutions by adsorption on bentonite, J. Colloid Interface Sci. 187 (1997) 338–343.
[6] R. Petrus, J. Warchol, Ion exchange equilibria between clinoptilolite and aqueous solutions of Na^+/Cu^{2+}, Na^+/Cd^{2+} and Na^+/Pb^{2+}, Micropor. Mesopor. Mater. 61 (2003) 137–146.
[7] M. Khraished, Y. Al-degs, W. Mcmin, Remediation of wastewater containing heavy metals using raw and modified diatomite, Chem. Eng. J. 99 (2004) 177–184.
[8] A. Dabrowski, Z. Hubicki, P. Podkoscielny, E. Robens, Selective removal of the heavy metal ions from waters and sewages by the ion-exchange method, Chemosphere 56 (2004) 91–106.
[9] M. Trgo, J. Peric, N.V. Medvidovic, Investigations of different kinetic models for zinc ions uptake by a natural zeolitic tuff, J. Environ. Manage. 79 (2006) 298–304.
[10] J. Rocha, M.W. Anderson, Microporous titanosilicates and other novel mixed octahedral-tetrahedral framework oxides, Eur. J. Inorg. Chem. (2000) 801–818.
[11] M.W. Anderson, O. Terasaki, T. Ohsuna, A. Philippou, S.P. MaeKay, A. Ferreira, J. Rocha, S. Lidin, Structure of the microporous titanosilicate ETS-10, Nature 367 (1994) 347–351.
[12] M.W. Anderson, O. Terasaki, T. Oshuna, P.J. O'Malley, A. Philippou, S.P. Mackay, A. Ferreira, J. Rocha, S. Lidin, Microporous titanosilicate ETS-10, a structural survey, Philos. Mag. B 71 (1995) 813–841.
[13] S.M. Kuznicki, K.A. Thrush, U.S. Patent 4,994,191 (1991).
[14] G.X.S. Zhao, J.L. Lee, P.A. Chia, Unusual adsorption properties of microporous titanosilicate ETS-10 toward heavy metal lead, Langmuir 19 (2003) 1977–1979.
[15] L.L. Lv, G. Tsoi, X.S. Zhao, Uptake equilibria and mechanisms of heavy metal ions on microporous titanosilicate ETS-10, Ind. Eng. Chem. Res. 43 (2004) 7900–7906.
[16] L. Lv, K. Wang, X.S. Zhao, Effect of operating conditions on the removal of Pb^{2+} by microporous titanosilicate ETS-10 in a fixed-bed column, J. Colloid Interface Sci. 305 (2007) 218–225.
[17] L. Al-Attar, A. Dyer, A. Paajanen, R. Harjula, Purification of nuclear wastes by novel inorganic ion exchangers, J. Mater. Chem. 13 (12) (2003) 2969–2974.
[18] J.H. Choi, S.D. Kim, Y.J. Kwon, W.J. Kim, Adsorption behaviors of ETS-10 and its variant, ETAS-10 on the removal of heavy metals, Cu^{2+}, Co^{2+}, Mn^{2+} and Zn^{2+} from a waste water, Micropor. Mesopor. Mater. 96 (2006) 157–167.
[19] C.C. Pavel, K. Popa, N. Bilba, A. Cecal, D. Cozma, A. Pui, The sorption of some radiocations on microporous titanosilicate ETS-10, J. Radioanal. Nucl. Chem. 258 (2) (2003) 243–248.
[20] A.I. Bortun, L.N. Bortun, A. Clearfield, Evaluation of synthetic inorganic ion exchangers for cesium and strontium removal from contaminated groundwater and wastewater, Solvent Extr. Ion Exch. 15 (5) (1997) 909–929.
[21] J.G. Decaillon, Y. Andrès, B.M. Mokili, J. Abbé, M. Tournoux, J. Patarin, Study of the ion exchange selectivity of layered titanosilicate $Na_3(Na,H)Ti_2O_2[Si_2O_6]22H_2O$, AM-4, for strontium, Solvent Extr. Ion Exch. 20 (2) (2002) 273–291.
[22] Y. Koudsi, A. Dyer, Sorption of 60Co on a synthetic titanosilicate analogue of the mineral penkvilksite-2O and antimonysilicate, J. Radioanal. Nucl. Chem. 247 (1) (2001) 209–219.
[23] C.B. Lopes, M. Otero, J. Coimbra, E. Pereira, J. Rocha, Z. Lin, A. Duarte, Removal of low concentration Hg^{2+} from natural waters by microporous and layered titanosilicates, Micropor. Mesopor. Mater. 193 (2007) 325–332.

[24] C.B. Lopes, P.F. Lito, M. Otero, Z. Lin, J. Rocha, C.M. Silva, E. Pereira, A. Duarte, Mercury removal with titanosilicate ETS-4: batch experiments and modelling, Micropor. Mesopor. Mater. 115 (2008) 98–105.
[25] C.B. Lopes, M. Otero, Z. Lin, C.M. Silva, E. Pereira, J. Rocha, A. Duarte, Mercury removal from aqueous solution using ETS-4—kinetic and equilibrium study, Chem. Eng. J. (2009), doi:10.1016/j.cej.2009.02.035.
[26] T.R. Ferreira, C.B. Lopes, P.F. Lito, M. Otero, Z. Lin, J. Rocha, E. Pereira, C.M. Silva, A. Duarte, Cadmium(II) removal from aqueous solution using microporous titanosilicate ETS-4, Chem. Eng. J. 147 (2009) 173–179.
[27] M.D. LeVan, G. Carta, C.M. Yon, Adsorption and ion exchange, in: D.W. Green (Ed.), Perry's Chemical Engineers' Handbook, Sect. 16, McGraw-Hill, New York, 1997.
[28] S. Lagergren, About the theory of so-called adsorption of soluble substances, Kungliga Svenska Vetenskapsakademiens, Handlingar 24 (1989) 1–39.
[29] C. Namasivayam, S. Senthilkumar, Removal of arsenic(V) from aqueous solution using industrial solid waste: adsorption rates and equilibrium studies, Ind. Eng. Chem. Res. 37 (1998) 4816–4822.
[30] Y.S. Ho, G. McKay, The sorption of lead(II) ions on peat, Water Res. 33 (1999) 578–584.
[31] G. McKay, Y.S. Ho, Pseudo-second order model for sorption processes, Process Biochem. 34 (1999) 451–465.
[32] Z. Reddad, C. Gerente, Y. Andres, P. Le Cloirec, Adsorption of several metal ions onto a low cost biosorbent: kinetic and equilibrium studies, Environ. Sci. Technol. 36 (2002) 2067–2073.
[33] M.F. Yardim, T. Budinova, E. Ekinci, N. Petrov, M. Razvigorova, V. Minkova, Removal of mercury (II) from aqueous solution by activated carbon obtained from furfural, Chemosphere 52 (2003) 835–841.
[34] N. Chiron, R. Guilet, E. Deydier, Adsorption of Cu(II) and Pb(II) onto a grafted silica: isotherms and kinetic models, Water Res. 37 (2003) 3079–3086.
[35] Z. Aksu, Application of biosorption for the removal of organic pollutants: a review, Process Biochem. 40 (2005) 997–1026.
[36] F.S. Zhang, J.O. Nriagu, H. Itoh, Mercury removal from water using activated carbons derived from organic sewage sludge, Water Res. 39 (2005) 389–395.
[37] F. Helfferich, Ion Exchange, Dover, NY, 1995.
[38] L. Liberti, G. Boari, R. Pasión, Chloride/sulfate exchange on anion resins. Kinetic investigations II. Particle diffusion rates, Dessalination 25 (2) (1978) 123–134.
[39] J.F. Rodrígez, J.L. Valverde, A.E. Rodrigues, Measurement of effective self-diffusion coefficients in a gel-type cation exchanger by the zero-length-column method, Ind. Eng. Chem. Res. 37 (1998) 2020–2028.
[40] J.L. Valverde, A. De Lucas, M. Carmona, M. González, J.F. Rodrígez, A generalized model for the measurement of effective diffusion coefficients of heterovalent ions in ion exchange by zero-length column method, Chem. Eng. Sci. 59 (2004) 71–79.
[41] R. Krishna, J.A. Wesselingh, Maxwell–Stefan approach to mass transfer, Chem. Eng. Sci. 52 (6) (1997) 861–911.
[42] C.M. Silva, P.F. Lito, Application of the Maxwell–Stefan approach to ion exchange in microporous materials. Batch process modeling, Chem. Eng. Sci. 62 (2007) 6939–6946.
[43] P.F. Lito, C.M. Silva, Comparison between Maxwell–Stefan and Nernst–Planck equations to describe ion exchange in microporous materials, Defect Diffus. Forum 273–276 (2008) 776–781.
[44] Decreto-Lei n. 236/98, 01-08-1998 (consulted on January 2009): http://bdjur.almedina.net/item.php?field=node_id&value=702871.
[45] P.M. Armenante, D.J. Kirwan, Mass transfer to microparticles in agitated systems, Chem. Eng. Sci. 44 (1989) 2781–2796.
[46] M.A. Fernandez, G. Carta, Characterization of protein adsorption by composite silica-polyacrylamide gel anion exchangers. I. Equilibrium and mass transfer in agitated contactors, J. Chromatogr. A 746 (1996) 169–183.
[47] A. Bhattacharya, Predicting rates of dissolution of polydisperse solids in reactive media, Chem. Eng. Process. 46 (2007) 573–583.
[48] J.H. Rushton, E.W. Costich, H.J. Everett, Power Characteristics of Mixing Impellers, John Willey, New York, 1968.
[49] S.K. Gupta, Momentum Transfer Operations, McGraw-Hill, New Delhi, 1979.
[50] W.E. Schiesser, The Numerical Method of Lines, Academic Press, USA, 1991.
[51] W.H. Lawton, E.A. Sylvestre, Elimination of linear parameters in nonlinear regression, Technometrics 13 (1971) 461–467.
[52] S.P. Mishra, V.K. Singh, D. Tiwari, Radiotracer technique in adsorption study: part XVII. Removal behaviour of alkali metal (K- and Li-) titanates for Cd(II), Appl. Radiat. Isot. 49 (12) (1998) 1467–1475.
[53] S. Kocaoba, Comparison of Amberlite IR 120 and dolomite's performances for removal of heavy metals, J. Hazard. Mater. 147 (2007) 488–496.
[54] A.M. El-Kamash, Evaluation of zeolite A for the sorptive removal of Cs+ and Sr2+ ions from aqueous solutions using batch and fixed bed column operations, J. Hazard. Mater. 151 (2008) 432–445.
[55] M. Sprynskyy, B. Buszewski, A.P. Terzyk, Study of the selection mechanism of heavy metal (Pb2+, Cu2+, Ni2+ and Cd2+) adsorption on clinoptilolite, J. Colloid Interface Sci. 304 (2006) 21–28.
[56] Y.S. Ok, J.E. Yang, Y. Zhang, S. Kim, D. Chung, Heavy metal adsorption by a formulated zeolite-Portland cement mixture, J. Hazard. Mater. 147 (2007) 91–96.
[57] E.N. Coker, L.V.C. Rees, Kinetics of ion-exchange in quasi-crystalline aluminosilicate zeolite precursors, Micropor. Mesopor. Mater. 84 (2005) 171–178.
[58] N.M. Brooke, L.V.C. Rees, Kinetics of ion-exchange. Part II.Trans, Trans. Faraday Soc. 65 (1969) 2728–2739.
[59] E.N. Coker, L.V.C. Rees, Ion exchange in beryllophosphate-G, J. Chem. Soc. Faraday Trans. 88 (1992) 273–276.
[60] I.A.M. Ahmed, S.D. Yong, N.M.J. Crout, Time-dependent sorption of Cd2+ on a CaX zeolite: experimental observations and model predictions, Geochim. Cosmochim. Acta 70 (2006) 4850–4861.